Critical behaviour of RMnO$_3$ (R = La, Pr, Nd) by thermal diffusivity and specific heat measurements

A Oleaga[1], **A Salazar**[1], **D Prabhakaran**[2] **and A T Boothroyd**[2]

[1] Departamento Física Aplicada I, Escuela Superior de Ingenieros, Universidad del País Vasco, Alameda Urquijo s/n, 48013-Bilbao, Spain
[2] Department of Physics, Clarendon Laboratory, University of Oxford, Oxford OX1 3PU, UK

E-mail: alberto.oleaga@ehu.es

Abstract
An ac photopyroelectric calorimeter has been used to measure the thermal diffusivity and specific heat of the perovskite manganites RMnO$_3$ (R = La, Pr, Nd) close to their magnetic transitions. Taking into account that the inverse of the thermal diffusivity has the same critical behaviour as the specific heat, the critical exponent α of the magnetic transition has been obtained by means of both magnitudes. The results in all cases are consistent with the Heisenberg model ($\alpha = -0.11$), irrespective of the rare-earth ion.

1. Introduction

Perovskite manganites R$_{1-x}$A$_x$MnO$_3$ (R = lanthanide, A = alkaline earth) have attracted great attention in the last years due to their colossal magnetoresistance [1–3]. Their electric, magnetic and thermal properties are determined by the strong interplay of magnetism, electron–lattice coupling and orbital and charge ordering, which is reflected in their rich and complex phase diagrams [3–6]. The presence of Sr, Ca, Ba instead of the trivalent rare-earth ion introduces holes in the Mn e$_g$ orbitals, influencing the superexchange between the Mn sites, giving place to double-exchange interactions and reducing Jahn–Teller-type distortions. As a consequence, several types of ordering phenomena appear, in different forms of antiferromagnetic or ferromagnetic insulators or metals.

In this study we are focusing our attention on the undoped parent compounds RMnO$_3$ (R = La, Pr, Nd). LaMnO$_3$ is by far the most studied. It presents a Jahn–Teller distorted orthorhombic structure below 800 K, and an antiferromagnetic (AFM) to paramagnetic (PM) transition at about 139 K, being an insulator in both phases [5]. The low-temperature phase is an orbitally ordered A-type AFM, displaying weak ferromagnetism due to the Dzialoshinski–Moriya interaction, i.e., a tiny canting of the spin from the orientation of a pure collinear antiferromagnet [7]. If La is substituted by isovalent Pr or Nd, there is a small change in the tolerance factor due to the smaller size of the ionic cations and a slight alteration of the cell

parameters (the remaining three compounds in the *Pbmn* space group) [3]. The electronic configuration of the Mn ions is qualitatively conserved and the orbitally ordered A-type AFM phase is maintained [8–10], but with some changes in the magnetic properties, which become apparent in the small ferromagnetic component along the *c*-axis: for Pr, the canting is of the same origin and order as that for La, but in Nd it is about 20 times stronger and is attributed to the Nd spins [10].

We are interested in the influence of the rare-earth substitution on the critical behaviour of the antiferromagnetic to paramagnetic transition, which will provide information on the magnetic properties of manganites. In a previous paper we dealt with the evolution of the critical behaviour in $La_{1-x}Sr_xMnO_3$ as hole doping was increased up to $x = 0.35$. Our results, based only on thermal diffusivity measurements, pointed to the Heisenberg model in the parent compound [11], in agreement with other authors [7, 12]. As far as we know, there are no studies of critical behaviour on $PrMnO_3$ or $NdMnO_3$, either based on magnetic or on thermal measurements.

The aim of this work is, on the one hand, to study the thermal properties of $RMnO_3$ (R = La, Pr, Nd), to which very little attention has been paid [13–17], and on the other hand, to study the critical behaviour of the magnetic transition through the critical exponent α, which is usually obtained by means of specific heat measurements. We have obtained it by two independent sources: thermal diffusivity and specific heat. Taking into account the relationship between specific heat c and thermal diffusivity D through the equation $c = \frac{K}{\rho D}$ (where ρ stands for density and K for thermal conductivity), the inverse of the thermal diffusivity has the same critical behaviour as the specific heat, provided that the thermal conductivity does not present singularities at the magnetic transitions.

2. Experimental techniques and fitting procedures

High-quality single crystals of $RMnO_3$ (R = La, Pr, Nd) were grown by the floating-zone technique. Detailed growing procedures have been reported elsewhere [18]. Slices of thickness between 0.35 and 0.45 mm were cut from the grown rods, perpendicular to the growth direction (*c*-axis) for this study.

Thermal diffusivity and specific heat measurements were performed by a high-resolution ac photopyroelectric calorimeter in the standard back-detection configuration [19, 20]. A mechanically modulated He–Ne laser beam of 5 mW illuminates the upper surface of the sample under study. Its rear surface is in thermal contact with a 350 μm thick $LiTaO_3$ pyroelectric detector with Ni–Cr electrodes on both faces, by using an extremely thin layer of a highly heat-conductive silicone grease (Dow Corning, 340 Heat Sink Compound). The photopyroelectric signal is processed by a lock-in amplifier in the current mode. Both sample and detector are placed inside a nitrogen bath cryostat that allows measurements in the temperature range from 77 to 500 K, at rates that vary from 100 mK min^{-1} for measurements on a wide temperature range to 10 mK min^{-1} for high-resolution runs close to the phase transitions.

The natural logarithm (ln V) and the phase (Ψ) of the normalized photopyroelectric current (that is obtained dividing by the signal provided by the bare detector) have a linear dependence on $\sqrt{f}$, with the same slope. From their slope m and from the vertical separation d the thermal diffusivity and the thermal effusivity ($e = \sqrt{\rho c K}$) of the sample can be obtained [21]:

$$D = \frac{\pi \ell^2}{m^2} \tag{1}$$

$$e = e_p \left(\frac{2}{\exp(d)} - 1 \right), \tag{2}$$

where ℓ is the sample thickness and e_p is the thermal effusivity of the pyroelectric detector. These equations are valid for opaque and thermally thick samples (ℓ is higher than the thermal diffusion length $\mu = \sqrt{D/\pi f}$). However, at temperatures below ≈ 230 K, where the coupling grease freezes, an important piezoelectric contribution is added to the pyroelectric signal, affecting the linearity of the dependence on $\sqrt{f}$. This contribution has been taken into account in order to obtain reliable values of D and e [22].

Once thermal diffusivity and effusivity have been measured at a certain reference temperature (T_{ref}, D_{ref}, e_{ref}), the temperature is changed while recording the amplitude and phase of the pyroelectric signal, at a fixed frequency (8 Hz in this study, performing heating runs). The temperature dependences of D and e are given by [21, 23]:

$$D(T) = \left[\frac{1}{\sqrt{D_{ref}}} - \frac{\Delta(T)}{\ell\sqrt{\pi f}} \right]^{-2} \tag{3}$$

$$e(T) = e_p(T) \left(\frac{1 + \frac{e_{ref}}{e_p(T_{ref})}}{\exp[\Delta''(T)]} - 1 \right), \tag{4}$$

where $\Delta(T) = \Psi(T) - \Psi(T_{ref})$, $\Delta'(T) = \ln V(T) - \ln V(T_{ref})$ and $\Delta''(T) = \Delta'(T) - \Delta(T)$. Finally, the temperature dependences of the specific heat and thermal conductivity are obtained:

$$c(T) = \frac{e(T)}{\rho\sqrt{D(T)}} \tag{5}$$

$$K(T) = e(T)\sqrt{D(T)}. \tag{6}$$

This technique is especially suited for the measurement of thermal properties around phase transitions, since small temperature gradients in the sample produce a good signal-to-noise ratio, letting thermal parameters be measured with high accuracy.

Concerning the fitting procedures, the specific heat and the inverse of the thermal diffusivity have been fitted to the same function with different parameters, the function which is generally used for specific heat [24, 25]:

$$c = B + Ct + A|t|^{-\alpha}(1 + E|t|^{0.5}) \tag{7}$$

$$1/D = G + Ht + F|t|^{-\alpha}(1 + I|t|^{0.5}) \tag{8}$$

where $t = (T - T_N)/T_N$ is the reduced temperature, T_N is the Néel temperature and A, B, C, E, F, G, H and I are adjustable parameters for $T > T_N$. Similar equations are used for $T < T_N$ with prime parameters. Following Marinelli and co-workers [25], in order to reduce the statistical correlation among set of parameters, the expressions used for our fittings were

$$c = B + C(T - T_N) + A^+|T - T_N|^{-\alpha}(1 + E^+|T - T_N|^{0.5}) \qquad T > T_N \tag{9a}$$

$$c = B + C(T - T_N) + A^-|T - T_N|^{-\alpha}(1 + E^-|T - T_N|^{0.5}) \qquad T < T_N \tag{9b}$$

$$1/D = G + H(T - T_N) + F^+|T - T_N|^{-\alpha}(1 + I^+|T - T_N|^{0.5}) \qquad T > T_N \tag{10a}$$

$$1/D = G + H(T - T_N) + F^-|T - T_N|^{-\alpha}(1 + I^-|T - T_N|^{0.5}) \qquad T < T_N. \tag{10b}$$

Provided that we consider $|T - T_N|$ as $|(T - T_N)/1K|$, the parameters in equations (7) and (8) and equations (9) and (10) have the same units; therefore, the same relations which apply among the parameters in the first group of equations hold for the second group.

The data were simultaneously fitted for $T > T_N$ and $T < T_N$ with a nonlinear least square routine. First of all, we selected a fitting range close to the peak while avoiding the rounding, and kept the value of T_N fixed. We obtained a first fitting without a correction to the scaling term and obtained a set of adjusted parameters. Afterwards, we tried to increase the
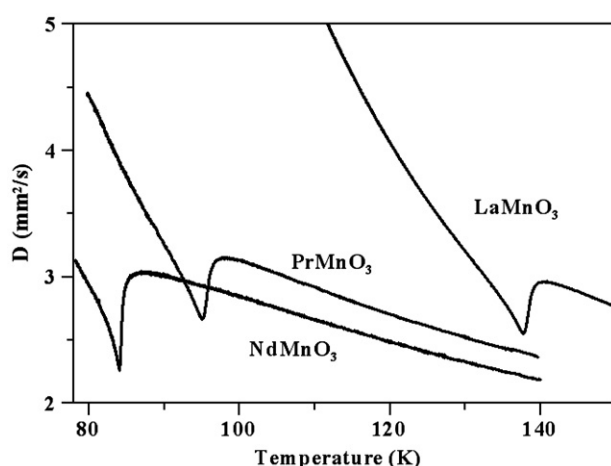
Figure 1. Thermal diffusivity D as a function of temperature showing the antiferromagnetic to paramagnetic transition. In all cases the dip minimum marks the Néel temperature.

number of points included in the fitting, first fixing t_{min} and increasing t_{max}, and then fixing t_{max} and decreasing t_{min}. The next step was introducing a correction to the scaling term, trying to improve the fitting. As a last check, we let T_N be a free parameter in order to confirm the fitting. In the whole process, we focused our attention on the rms deviations as well as on the deviation plots, which are plots of the differences between the fitted values and the measured ones as a function of the reduced temperature. The values of T_N were the same both for specific heat and the inverse of thermal diffusivity.

3. Experimental results and discussion

To begin with, thermal diffusivity was measured for the three samples, at room temperature. The values obtained are 1.37 ± 0.03 mm^2 s^{-1} for LaMnO$_3$, 1.35 ± 0.03 mm^2 s^{-1} for PrMnO$_3$, and 1.67 ± 0.04 mm^2 s^{-1} for NdMnO$_3$. Differences in thermal diffusivity or thermal conductivity at room temperature in pure manganites due to the changing of the rare-earth ion should be minor; as the averaged ionic radius decreases from La to Pr, then to Nd, the tolerance factor is reduced and so there is a change in the cell parameters, getting further away from the perfect cubic perovskite structure. But, nevertheless, all three manganites crystallize in the *Pbnm* space group with cell parameters quite close to each other. As thermal conduction in manganites is mainly governed by phonons [26], the thermal conduction mechanisms are not altered by the changing of the rare earth; at most, the phonon mean free path may be slightly altered, so at room temperature (far away from the antiferromagnetic to paramagnetic transition) the values for thermal diffusivity must be quite similar. The reason why in NdMnO$_3$ a slightly higher value is obtained might be that this particular crystal is of a better quality than the other two. It is well known that the measured values for thermal diffusivity depend on the quality of the crystal (stoichiometrically and crystallographically): the better the quality, the higher the measured thermal diffusivity value. In this way, Hemberger *et al* affirm that NdMnO$_3$ has a higher stoichiometric stability than LaMnO$_3$ [10]. Moreover, the fact that the dip at the antiferromagnetic to paramagnetic transition is sharper than in the case of PrMnO$_3$ and LaMnO$_3$ (see figure 1) also supports this hypothesis. The higher the quality of the crystal, the sharper the experimental peaks are.
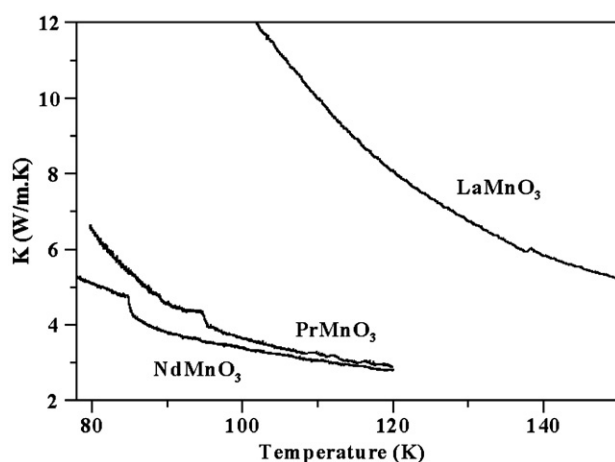
Figure 2. Thermal conductivity K as function of temperature showing the antiferromagnetic to paramagnetic transition.

The temperature dependence of the thermal diffusivity around the antiferromagnetic to paramagnetic transition is shown in figure 1. The dip defines the Néel temperature T_N (137.3 K, 94.9 K and 84.0 K for LaMnO$_3$, PrMnO$_3$ and NdMnO$_3$ respectively). It is worth emphasizing that the exact position of T_N for a given manganite depends on the quality of the crystal, as the dispersion of the results among different authors using different crystals reveals [10]. In the region below the transition ($T < T_N$), thermal diffusivity strongly decreases as the temperature is raised due to the reduction in phonon mean free path by phonon–phonon scattering. At $T > T_N$ thermal diffusivity smoothly decreases. The presence of the magnetic transition is to superimpose a dip on the thermal diffusivity curve, creating an analogous effect as it has on the specific heat curves.

Figure 2 shows the thermal conductivity K as a function of temperature. Note that as thermal conductivity is calculated using both the phase and the amplitude of the photopyroelectric signal, the result is a bit noisier than in the case of the diffusivity curves, where only the phase is needed. In all three cases there is a monotonic decrease as the temperature is raised, with no singularities at the Néel temperature, but at most a simple step while changing from the antiferromagnetic to the paramagnetic phase. These results are in agreement with experimental results obtained by other authors in the case of LaMnO$_3$ [5, 16]. The absence of singularities means that, indeed, the same critical behaviour can be expected from $1/D$ and from c.

To obtain the critical parameters, detailed measurements of D and c were performed in the near vicinity of T_N. These results are shown by circles in figure 3, where $1/D$ and c are depicted as a function of the reduced temperature $t = (T - T_N)/T_N$. Both magnitudes present in the three samples the characteristic lambda-shape of a second-order phase transition. The results of the fittings to equations (9) and (10) are presented in tables 1 and 2 and shown by the continuous line in figure 3. They are all quite good fits, as can be seen in the residual R values (very close to 1), in the parameter errors and in the small deviation of the fitted curves from the experimental data. However, our results are limited by how close we can get to T_N in the fitting; there is a deviation of the data from the predicted power law for small reduced temperatures, this fact being determined by the peak rounding. The minimum limit of the fitting ranges (both above and below T_N) is the inflexion point of the curves, in which the rounding begins.
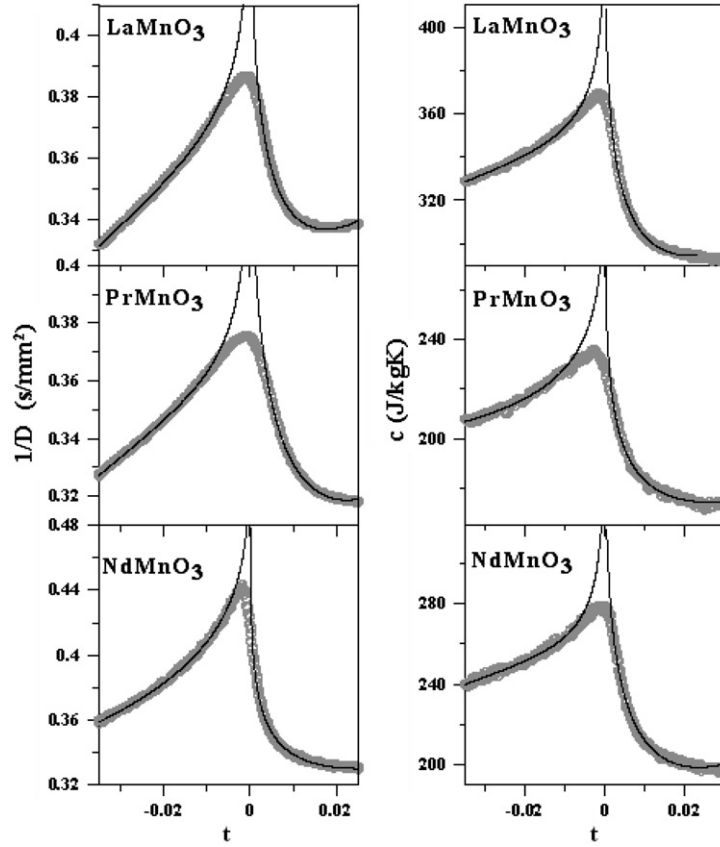
Figure 3. Inverse of the thermal diffusivity and specific heat as a function of the reduced temperature $t = (T - T_N)/T_N$ in the near vicinity of the Néel temperature. The circles represent the experimental points (not all are shown), the continuous lines the fitted functions.

Table 1. Results of the fitting for the inverse of the thermal diffusivity, including the critical exponent, range of the fitting, adjustable parameters and deviation coefficients.

	LaMnO$_3$	PrMnO$_3$	NdMnO$_3$
α	-0.10 ± 0.01	-0.11 ± 0.01	-0.11 ± 0.01
F^+/F^-	1.02	0.95	1.43
$t_{min}-t_{max}$ ($T < T_N$)	9.5×10^{-3}–3×10^{-2}	9.5×10^{-3}–3.3×10^{-2}	7.1×10^{-3}–4.3×10^{-2}
$t_{min}-t_{max}$ ($T > T_N$)	2.9×10^{-3}–2.5×10^{-2}	3.9×10^{-3}–2.4×10^{-2}	1.1×10^{-3}–3.4×10^{-2}
F^+ (s mm^{-2})	-0.37 ± 0.03	-0.40 ± 0.03	-0.27 ± 0.05
G (s mm^{-2})	0.71 ± 0.03	0.70 ± 0.03	0.69 ± 0.05
H (s mm^{-2})	0.0181 ± 0.0004	0.034 ± 0.001	0.002 ± 0.001
I^+	-0.14 ± 0.01	-0.24 ± 0.02	0.02 ± 0.01
I^-	0.006 ± 0.002	0.064 ± 0.008	-0.11 ± 0.02
R	0.997 76	0.999 55	0.998 96

This rounding is inherent to the samples and not attributable to the measurement technique, as studies on other materials have established [26].

The results that have been obtained give a coherent picture of the critical behaviour of the undoped manganites RMnO$_3$ (R = La, Pr, Nd). From the values of the critical exponents

Table 2. Results of the fitting for the specific heat, including the critical exponent, range of the fitting, adjustable parameters and deviation coefficients.

	LaMnO$_3$	PrMnO$_3$	NdMnO$_3$
α	-0.11 ± 0.01	-0.11 ± 0.02	-0.11 ± 0.02
A^+/A^-	1.07	1.21	1.01
$t_{\min}-t_{\max}$ ($T < T_N$)	8.2×10^{-3}–3.6×10^{-2}	9.5×10^{-3}–3.5×10^{-2}	8.4×10^{-3}–4.4×10^{-2}
$t_{\min}-t_{\max}$ ($T > T_N$)	1.6×10^{-3}–2.5×10^{-2}	1.7×10^{-3}–2.4×10^{-2}	2.5×10^{-3}–2.8×10^{-2}
A^+ (J kg^{-1}K^{-1})	-370 ± 39	-259 ± 66	-458 ± 74
B (J kg^{-1}K^{-1})	688 ± 39	466 ± 65	647 ± 88
C (J kg^{-1}K^{-1})	14.4 ± 0.05	4.7 ± 0.6	30 ± 2
E^+	-0.16 ± 0.02	-0.10 ± 0.02	-0.22 ± 0.04
E^-	-0.013 ± 0.002	-0.08 ± 0.02	0.019 ± 0.007
R	0.9987	0.997 56	0.9976

obtained, a 3D-Heisenberg behaviour ($\alpha = -0.115$ and $A^+/A^- = 1.5$ as theoretical values) can be attributed to these undoped manganites, suggesting that the interactions among spins are short-ranged, ruling out other possible descriptions based on mean-field models. Actually, a critical exponent $\alpha = -0.11$ has been found for the three samples, both from $1/D$ and from c measurements. However, the ratio A^+/A^- is lower than the theoretical one. This result may point to a deviation of the critical behaviour of these manganites from a perfect Heisenberg model. This fact was suggested by Moussa and co-workers in the case of LaMnO$_3$, where a small anisotropy term had to be included in the Heisenberg Hamiltonian in order to account for a smaller value in the experimental critical exponent for magnetization than theoretically expected [12].

Our aim is to extend this study to other RMnO$_3$ manganites; not only to those which maintain orthorhombic symmetry (Sm, Eu), but also to those which crystallize in a hexagonal structure (Ho, Er, Sc, Y), in order to see whether the Heisenberg universality is still more general.

Acknowledgment

References

[1] Salamon M B and Jaime M 2001 *Rev. Mod. Phys.* **73** 583
[2] Dagotto E, Hotta T and Moreo A 2001 *Phys. Rep.* **344** 1
[3] Tokura Y and Tomioka Y 1999 *J. Magn. Magn. Mater.* **200** 1
[4] Urushibara A, Moritomo Y, Arima T, Asamitsu A, Kidon G and Tokura Y 1995 *Phys. Rev.* B **51** 14103
[5] Zhou J S and Goodenough J B 2001 *Phys. Rev.* B **64** 024421
[6] Kuwahara H, Kawasaki R, Hirobe Y, Kodama S and Kakishima A 2003 *J. Appl. Phys.* **93** 7367
[7] Cestelli Guidi M, Allodi G, De Renzi R, Guidi G, Hennion M, Pinsard L and Amato A 2001 *Phys. Rev.* B **64** 064414
[8] Wu S Y, Kuo C M, Wang H Y, Li W H, Lee K C, Lynn J W and Liu R S 2000 *J. Appl. Phys.* **87** 5822
[9] Muñoz A, Alonso J A, Martínez-Lope M J, García-Muñoz J L and Fernández-Díaz M T 2000 *J. Phys.: Condens. Matter* **12** 1361
[10] Hemberger J, Brando M, Wehn R, Ivanov V Yu, Mukhin A A, Balbashov A M and Loidl A 2004 *Phys. Rev.* B **69** 064418
[11] Oleaga A, Salazar A, Prabhakaran D and Boothroyd A T 2004 *Phys. Rev.* B **70** 184402

A Oleaga *et al*

[12] Moussa F, Hennion M, Rodriguez-Carvajal J, Moudden J H, Pinsard L and Revcolevschi A 1996 *Phys. Rev.* B **54** 15149
[13] Satoh H, Takagi M, Kinukawa K and Kamegashira N 1999 *Thermochim. Acta* **299** 123
[14] Klopkin M N, Paniva G Kh, Shikov A A, Sinyavskii V F and Shulyatev D A 2000 *Phys. Solid State* **42** 114
[15] Liu G L, Zhou J S and Goodenough J B 2001 *Phys. Rev.* B **64** 144414
[16] Cohn J L, Neumeier J J, Popoviciu C P, McClellan K J and Leventouri Th 1997 *Phys. Rev.* B **56** 56
[17] Fujishiro H, Ikebe M, Akashi T and Goto T 2002 *Physica* B **316/317** 261
[18] Prabhakaran D, Coldea A I, Boothroyd A T and Blundell S J 2002 *J. Cryst. Growth* **237–239** 806
[19] Marinelli M, Zammit U, Mercuri F and Pizzoferrato R 1992 *J. Appl. Phys.* **72** 1096
[20] Chirtoc M, Dadarlat D, Bicanic D, Antoniow J S and Egée M 1997 *Progress in Photothermal and Photoacoustic Science and Technology* vol 3, ed A Mandelis and P Hess (Bellingham, WA: SPIE Optical Engineering Press)
[21] Delenclos S, Chirtoc M, Hadj Sahraoui A, Kolinsky C and Buisine J M 2002 *Rev. Sci. Instrum.* **73** 2773
[22] Salazar A and Oleaga A 2005 *Rev. Sci. Instrum.* **76** 034901
[23] Salazar A 2003 *Rev. Sci. Instrum.* **74** 825
[24] Kornblit A and Ahlers G 1975 *Phys. Rev.* B **11** 2678
[25] Marinelli M, Mercuri F, Zammit U, Pizzoferrato R, Scudieri F and Dadarlat D 1994 *Phys. Rev.* B **49** 9523
[26] Salazar A, Oleaga A and Prabhakaran D 2004 *Int. J. Thermophys.* **25** 1269